An RGD small-molecule integrin antagonist induces detachment-mediated anoikis in glioma cancer stem cells

MAYRA PAOLILLO[1], MARISA C. GALIAZZO[1], ANTONIO DAGA[2], EMILIO CIUSANI[3], MASSIMO SERRA[1], LINO COLOMBO[1] and SERGIO SCHINELLI[1]

[1]Department of Drug Sciences, University of Pavia, I-27100 Pavia; [2]Institute for Research, Hospitalization and Care-University Hospital (IRCCS-AOU) San Martino-Cancer Research Institute (IST), I-16132 Genoa; [3]Fondazione IRCCS Neurological Institute C. Besta, I-20133 Milan, Italy

Received April 16, 2018; Accepted August 20, 2018

DOI: 10.3892/ijo.2018.4583

Abstract. The malignancy of glioblastoma (GB) is primarily due to the ability of glioma cancer stem cells (GSC) to disseminate into surrounding brain tissues, despite surgery and chemotherapy, and to form new tumoral masses. Members of the RGD-binding integrin family, which recognize the arginine-glycine-aspartic acid (RGD) sequence present in components of the extracellular matrix, and which serve a crucial function in the dissemination of GCS, are overexpressed in GB. Small-molecule integrin antagonists (SMIAs) designed to recognize RGD-integrins may therefore be an effective tool for decreasing GB infiltration and recurrence. In the present study, *in vitro* pro-apoptotic and infiltrative effects elicited by the SMIA 1a-RGD in human GSC were investigated. Reverse transcription-quantitative polymerase chain reaction analysis revealed that, compared with normal human astrocytes, GSC grown on laminin-coated dishes overexpressed stemness markers as well as αvβ3 and αvβ5 integrins. In addition, dissociated GSC were identified to exhibit tumorigenic capacity when injected into immunodeficient mice. Using annexin/fluorescence-activated cell sorting analysis and ELISA nucleosome assays, it was identified that treatment of GSC with 25 μM 1a-RGD for 48 h elicited detachment-dependent anoikis not accompanied by necrosis-dependent cell death. A colorimetric proliferation assay indicated that 1a-RGD did not affect cell viability, but that, instead, it markedly inhibited GSC migration as assessed using a Transwell assay. Western blot experiments revealed a decrease in focal adhesion kinase and protein kinase B phosphorylation with a concomitant increase in caspase-9 and -3/7 activity following 1a-RGD treatment, suggesting that the pro-anoikis effects of 1a-RGD may be mediated by these molecular mechanisms. Western blot analysis revealed no changes in specific markers of autophagy, suggesting further that 1a-RGD-induced cell death is primarily sustained by anoikis-associated mechanisms. In conclusion, the results of the present study indicate that SMIA have potential as a therapeutic tool for decreasing GSC dissemination.

Correspondence to: Dr Mayra Paolillo, Department of Drug Sciences, University of Pavia, 12 Viale Taramelli, I-27100 Pavia, Italy
E-mail: mayra.paolillo@unipv.it

Key words: glioma cancer stem cells, glioblastoma, caspase, cell migration, anoikis, autophagy, integrin antagonist

Introduction

The principal issue in the therapy of glioma is the recurrence, even following surgical debulking combined with radio- or chemotherapy, of newly formed solid masses in other distant areas of the brain. These recurrences are due to glioma cells that detach from the original tumor mass and disseminate in the brain parenchyma to establish new tumoral niches. The relatively poor advancement in glioma therapy in the last decades may be partly due to the lack of suitable *in vitro* and *in vivo* glioma models. The most reliable *in vitro* glioma model is currently provided by glioma stem cells (GSC), a subpopulation of glioma cells that, when propagated in culture in the absence of serum as neurospheres or adherent cells plated over laminin, retain their original genotype and phenotype (1). GSC are characterized by tumorigenicity, chemoresistance, radioresistance and infiltrative ability, making them crucial targets for therapeutic strategies.

Since glioma recurrence primarily involves mechanisms associated with cell detachment and attachment (2), extracellular matrix (ECM)-binding proteins expressed on cell membranes, such as integrins, have been intensively exploited as potential targets to counteract glioma malignancy.

Certain RGD-binding integrins, particularly αvβ3, αvβ5 and α5β1, are overexpressed in glioma cells compared with normal brain tissues. They have also been identified to be expressed by non-tumoral cell types present in the tumoral niche, such as proliferating vascular endothelial cells and pericytes (2). In *in vitro* and *in vivo* animal models, the prototype RGD-integrin antagonist cilengitide and other structurally related small-molecule integrin antagonists (SMIA) were identified to modulate migration and apoptotic processes in glioma cell lines (3-5). However, the promising results obtained using

cilengitide were not confirmed in clinical trials, prompting efforts to synthesize SMIA with different chemical structures and pharmacological properties.

These compounds have primarily been tested on glioma and other cancer cell lines grown in the presence of serum, and, although the function of integrins and periostin in gliomas has been well-characterized (6), the expression pattern of RGD-binding integrins and their function in regulating glioma cell infiltration in the GSC model remain unclear.

In an attempt to rectify this deficit in our knowledge, the functional effects elicited by SMIA-integrin binding in modulating the ECM-integrin interaction and the subsequent effects elicited by 1a-RGD on integrin-dependent signal transduction pathways in three human GSC lines grown in serum-free medium and plated on laminin coated dishes were investigated.

The results of the present study indicated that 1a-RGD decreases cell migration and induces cell detachment and caspase-dependent anoikis in detached GSC, thus highlighting the important potential of SMIA to decrease the malignant dissemination of GSC.

Materials and methods

Synthesis of 1a-RGD. 1a-RGD was synthesized as described previously (7), by means of a solution-phase method that exploited the benzyloxycarbonyl protection strategy. The binding of 1a-RGD to integrin receptors was determined using *in vitro* binding assays, and its half-maximal inhibitory concentration (IC_{50}) values for αvβ3 and αvβ5 were identified to be 6.4 and 7.7 nM, respectively (7). The integrin antagonist 1a-RGD was solubilized in PBS at a concentration of 2 mM, and for the treatments it was diluted in the GSC growth medium to a final concentration of 25 μM.

Cell culture. Samples designated GSC3, GSC4 and GSC7 were isolated from tumor tissue in the Neurosurgery Department at the Institute for Research, Hospitalization and Care-University Hospital (IRCCS-AOU) San Martino-Cancer Research Institute (IST) (Genoa, Italy) following informed consent, according to European Union legislation on informed consent and The Declaration of Helsinki, from the patients and Institutional Ethical Committee (IRCCS San Martino-IST) approval. The donor patients were undergoing brain surgery for the first time. Patients had never received previous radio- or chemotherapy and their tumors were classified by the pathologists as glioblastoma (GB) grade IV (World Health Organization classification). Clinicopathological characteristics are presented in Table I.

Primary cell cultures were established as described previously (8). Briefly, tumor samples were collected immediately following surgery, washed and mechanically dissociated. Primary cultures were grown in Dulbecco's modified Eagle's medium (DMEM)/Ham's F12 and neurobasal medium (1:1) (Gibco; Thermo Fisher Scientific, Inc., Waltham, MA, USA) with added GlutaMAX™ (Gibco; Thermo Fisher Scientific, Inc.), 100 μg/ml penicillin/streptomycin, 1% B-27 and N2 supplements (Gibco; Thermo Fisher Scientific, Inc.), 10 ng/ml basic fibroblast growth factor (bFGF) and 20 ng/ml epidermal growth factor (EGF) (PeproTech, Inc., Rocky Hill, NJ, USA). For routine culture, cells were plated at 20,000 cells/cm^2 on laminin-coated vessels [10 μg/ml laminin-1 (Sigma-Aldrich; Merck KGaA, Darmstadt, Germany) in PBS for 6-12 h], passaged at 70% confluence using Accutase dissociation reagent (Sigma; Merck KGaA) and split at a 1:3 ratio. The cells were used in experiments up to but not beyond the fifth passage *in vitro*. The GSC lines used were characterized at the outset for their tumorigenic properties by orthotopically xenografting 10,000 cells into the striatum of 6-8-week-old female non-obese diabetic/severe combined immunodeficient mice (average weight, 30 g each). For each glioblastoma cell line, 4 mice were used, under standard housing conditions (27˚C, 50% humidity,12-h light/12-h dark cycle), with free access to food and water (Table I).

All experiments involving animals were performed at IRCCS-AOU San Martino-IST in compliance with the guidelines approved by the Italian Ministry of Health and the Committee for Animal Well-Being in Cancer Research.

Normal human astrocytes (NHA) were purchased from Thermo Fisher Scientific, Inc. and grown in Astrocyte Medium (Gibco; Thermo Fisher Scientific, Inc.) in the presence of 10% fetal bovine serum (FBS; Gibco; Thermo Fisher Scientific, Inc.), according to the manufacturer's protocol. NHA were used for experiments not beyond the fifth *in vitro* passage and, 24 h before the experiments, the medium was replaced with the same medium used for GSC cultures to standardize experimental conditions.

Phenotypic characterization of GSC and their modification following in vitro differentiation: GSC differentiation in vitro. GSC cultures were seeded on Matrigel-coated glass coverslips and maintained for 2 weeks in DMEM/Ham's F12 supplemented with 2 mM L-glutamine, 50 IU/ml penicillin/50 μg/ml streptomycin and 10% FBS.

Phenotypic characterization of GSC and their modification following in vitro differentiation: Immunocytochemistry. GSC and their differentiated counterparts plated onto laminin-coated glass coverslips were fixed with 4% paraformaldehyde, permeabilized with PBS/0.1% Triton X-100, and stained with the following primary antibodies: Mouse monoclonal anti-nestin (1:1,000; cat. no. MAB1259; Novus Biologicals, Ltd., Cambridge, UK), rabbit anti-microtubule-associated protein 2 (MAP2; 1:1,000; cat. no. PA5-17646; Chemicon International; Thermo Fisher Scientific, Inc.), rabbit anti-glial fibrillary acidic protein (GFAP; 1:10,000; cat. no. Z0334; Dako; Agilent Technologies, Inc., Santa Clara, CA, USA) and rabbit anti-sex-determining region Y box 2 (SOX2; 1:500; cat. no. AB5603; EMD Millipore, Billerica, MA, USA). Immunocomplexes were detected with secondary fluorescent antibodies DyLight 488-conjugated goat anti-mouse immunoglobulin G (IgG) (cat. no. 111-545-003) and DyLight 594-conjugated goat anti-rabbit IgG (cat. no. 111-585-003) (Jackson ImmunoResearch Laboratories, Inc., West Grove, PA, USA). Cells were counterstained with Hoechst 33342 dye (Sigma-Aldrich; Merck KGaA) to identify all nuclei. Images were captured by automated Zeiss AxioImager M2 equipped with an Axiocam MRM (Zeiss GmbH, Jena, Germany). Results are presented as the percentage of stained cells from randomly selected fields.

Table I. Clinicopathological characteristics of patients and GSC tumorigenic potential in mice.

GSC line	Sex	Age, years	WHO grade	Type	Subtype	OS, months	Mouse survival, days
3	Male	48	IV	Primary	Neural	14.4	120
4	Male	78	IV	Secondary	Classical	13.5	80
7	Male	71	IV	Primary	ND	3.6	75

GSC, glioma cancer stem cell; WHO, World Health Organization; OS, overall survival; ND, not determined.

Table II. Primers used to amplify RGD-binding integrin mRNA in reverse transcription-quantitative polymerase chain reaction experiments.

Gene	Accession no.	Primer sequence (5'-3')
αv	NM_002210	F: actggcttaagagagggctgtg R: tgccttacaaaaatcgctga
β3	NM_000212	R: tcctcaggaaaggtccaatg R: tcctcaggaaaggtccaatg
β5	NM_002213	F: agcctatctccacgcacact R: cctcggagaaggaaacatca
α5	NM_002205	F: cctgctgtccaccatgtcta R: ttaatggggtgattggtggt
β1	NM_133376	F: tccaatggcttaatttgtgg R: cgttgctggcttcacaagta
RPL6	NM_001024662.1	F: agattacggagcagcagcgcaagattg R: gcaaacacagatcgcaggtagccc

F, forward; R, reverse; RPL6, ribosomal protein L6.

Reverse transcription-quantitative polymerase chain reaction (RT-qPCR). For mRNA expression analysis, RNA was extracted from GSC and NHA using QIAzol (Qiagen, Inc., Valencia, CA, USA), followed by digestion with DNase I (cat. no. D4263; Sigma-Aldrich; Merck KGaA) digestion step. RNA quality was assessed by determining the A_{260}/A_{280} ratio and the concentration was estimated at 260 nm. The primers were designed using Primer3 Input software (version 0.4.0; National Center for Biotechnology Information, Bethesda, MD, USA) and the specificity of each primer was checked by BLAST analysis (www.ncbi.nlm.nih.gov/tools/primer-blast). Primers used for integrin subunits and for the housekeeping gene ribosomal protein L6 (RPL6) in RT-qPCR have been reported previously (3) and are presented in Table II; primers used to amplify stemness-related mRNAs (9) are presented in Table III. PCR experiments were performed using the QuantiTect SYBR Green kit (Qiagen, Inc.) containing 10 μl 2X master mix, 1 μl each of 10 μM (0.4 μM) forward and reverse primer, 1 μl template cDNA and 7 μl nuclease-free water to a total volume of 20 μl, according to the manufacturer's protocol. Each assay was run with no template control. Cycling conditions were 95˚C for 15 min; then 40 cycles of 95˚C for 15 sec, 60˚C for 30 sec and 72˚C for 30 sec. At the end of the PCR, a melting curve analysis was performed to check for the presence of primer-dimers. Experiments were performed on three different cell preparations and each run was analyzed in duplicate.

Data are expressed as the fold increase in each gene in GSC compared with NHA, using the $2^{-\Delta\Delta Cq}$ method (10) following normalization to the RPL6 housekeeping gene.

Fluorescence-activated cell sorting (FACS) analysis. The expression of αvβ3, αvβ5 and α5β1 on cell membranes was determined using FACS analysis with antibodies directed against the integrin receptors. Briefly, following gentle detachment of the cells using a 1 mM EDTA/PBS solution to preserve the integrity of membrane proteins, cells were pelleted at 800 x g for 10 min and resuspended in 1 ml PBS to obtain a suspension of 20,000 cells/ml. The cell suspension was then incubated with the following antibodies (1 μg/ml): Mouse monoclonal anti-integrin αvβ3 antibody (cat. no. MAB1976; Merck KGaA), Alexa Fluor 633-conjugated goat anti-mouse (cat. no. A21050; Thermo Fisher Scientific, Inc.), fluorescein isothiocyanate (FITC)-conjugated mouse monoclonal anti-integrin αvβ5 antibody (cat. no. MAB1961F; Merck KGaA) and FITC-conjugated mouse monoclonal anti-integrin α5 antibody (cat. no. CBL497F; Merck KGaA).

To determine apoptosis, an Annexin V-binding assay was used (Annexin V-FITC Apoptosis Detection kit; eBioscience; Thermo Fisher Scientific, Inc.), according to the

Table III. Primers used to amplify stemness-associated mRNAs in reverse transcription-quantitative polymerase chain reaction assays.

Gene	Accession no.	Primer sequence (5'-3')
CD133	NM_006017.2	F: ccaccgctctagatactgctg R: cctatgccaaaccaaaacaaa
OCT4	NM_002701.4	F: ggtccgagtgtggttctgtaa R: atagcctggggtaccaaaatg
MUSASHI	NM_002442.3	F: actgaagtttcccaccaggat R: actgttcatgaaggtccaacg
NANOG	NM_024865.2	F: cagtctggacactggctgaa R: ctcgctgattaggctccaac
BMI1	NM_005180.6	F: ggaaagcaggcaagacttttt R: caaactatggcccaatgctta
NESTIN	NM_006617.1	F: gggacaagagaacctggaaac R: ggttcacttccacagactcca
SOX2	NM_003106	F: ggacttctttttgggggacta R: gcaaacttcctgcaaagctc
EZH2	NM_152998.1	F: tgccattgctaggttaattgg R: acaaccggtgtttcctcttct

manufacturer's protocol. Following treatments, spontaneously detached cells were recovered and stored separately, whereas attached cells were detached using 1 mM EDTA/PBS solution as aforementioned. The suspensions of attached and detached cells were centrifuged at 800 x g for 10 min, and the pellets were suspended in 1 ml Annexin V buffer, according to the manufacturer's protocol. FITC-conjugated Annexin V was added and cells were incubated for 15 min at room temperature. Following the addition of propidium iodide (PI), samples were acquired using a FACSVantage SE instrument (BD Biosciences, Franklin Lakes, NJ, USA) and analyzed using CellQuest software (version 5.1; BD Biosciences). At least 10,000 events per sample were recorded. Each experiment was performed three times.

Cell viability assays. Cells were plated in a 96-well plate (10,000 cells/100 μl per well) and treated with DMEM/Ham's F12 and neurobasal medium (1:1) containing 25 μM 1a-RGD for 8, 24 and 48 h. Following treatment, 20 μl MTS reagent (CellTiter 96 AQueous One Solution Cell Proliferation assay; Promega Corporation, Madison, WI, USA) was added to each well. After 3 h of incubation at 37˚C, the absorbance was determined in a multi-well plate reader at 450 nm. For each experimental point, eight wells were used and each independent experiment was performed three times.

The cell viability results were normalized to time-point-matched controls; 1a-RGD stock solution (200 mM in PBS) was diluted in the growth medium and added to the wells. In control wells, only the growth medium was added.

Cell migration assays. GSC (20,000 cells/well) were plated in culture medium lacking growth factors on a MaxGel (Sigma-Aldrich; Merck KGaA)-coated Transwell (Costar; Corning Incorporated, Corning, NY, USA). As chemoattractants, 500 μl EGF (20 ng/ml) and bFGF (10 ng/ml)-containing medium were placed under the Transwell membranes. The migration assay was performed for 8 h in the presence or absence of 25 μM 1a-RGD. Following removal of the MaxGel, the cells present on the lower side of the membrane were stained with DAPI (Sigma-Aldrich; Merck KGaA) and enumerated using a fluorescence microscope. For each membrane, 10 fields were observed. Each experiment was performed at least three times.

Western blot analysis. Cells grown in 60 mm diameter dishes were treated for the indicated times with 25 μM 1a-RGD. The cells were then rinsed twice in ice-cold PBS, and 200 ml cell lysis buffer [50 mM Tris/HCl pH 7.4, 1% (v/v) NP40, 0.25% (w/v) sodium deoxycholate, 1 mM phenylmethylsulfonyl fluoride, 1 mM Na_3VO_4, 1 mM EDTA, 30 mM sodium pyrophosphate, 1 mM NaF, 1 mg/ml leupeptin, 1 mg/ml pepstatin A, 1 mg/ml aprotinin and 1 mg/ml microcystin] was added to the dishes. Following scraping, the cells were sonicated for 10 min and centrifuged at 12,000 x g for 5 min at 4˚C. The amount of proteins in the supernatant was then determined using a Bicinchoninic Acid Protein assay kit (Pierce; Thermo Fisher Scientific, Inc.). For western blot analysis, 30 μg proteins were separated by SDS-PAGE (10% gel) at 150 V for 2 h and blotted onto 0.22 mm nitrocellulose membranes at 50 mA for 16 h. The membranes were first blocked for 2 h in Tris-buffered saline containing Tween-20 (TBST; 10 mM Tris/HCl, 150 mM NaCl and 0.1% Tween-20) containing 5% non-fat dry milk powder (TBSTM) and then incubated with the appropriate antibody [anti-phospho-FAK rabbit polyclonal antibody (cat. no. 3283); anti-phospho-Akt rabbit polyclonal antibody (cat. no. 9271); Cell Signaling Technology, Inc., Danvers, MA, USA] diluted 1:1,000 in TBSTM at 4˚C for 16 h with gentle agitation. The membranes were rinsed three times in TBST and then incubated

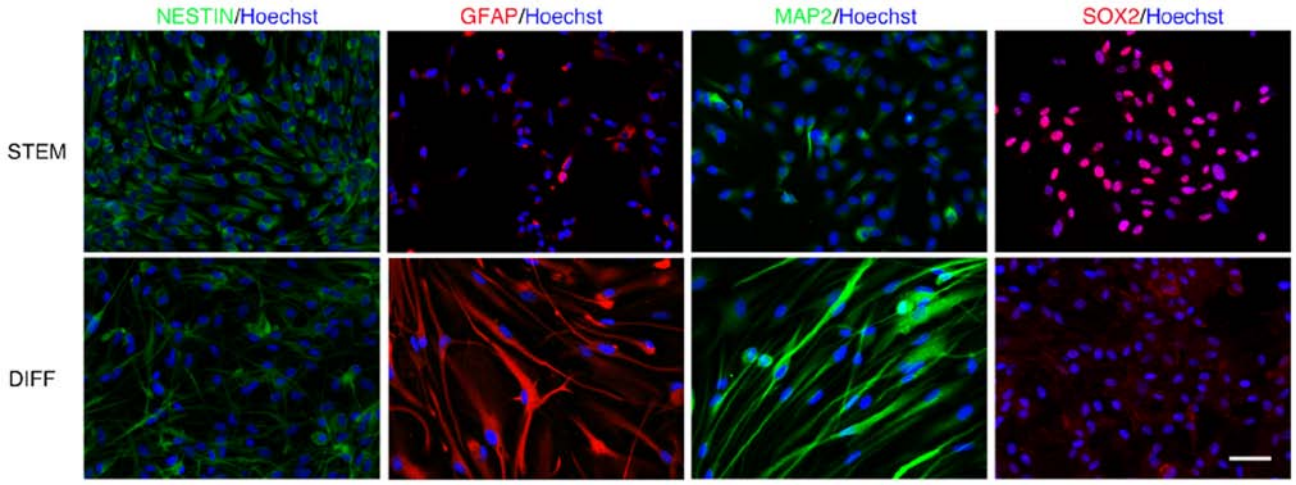

Figure 1. Expression of nestin, MAP2, GFAP and SOX2 in stemness and differentiating conditions in GSC3. GSC3 grown under stemness and differentiating conditions were stained using antibodies directed against stemness and differentiation markers. Nestin and SOX2 appeared to be predominantly expressed in undifferentiated GSC, whereas MAP2 and GFAP appeared to be primarily expressed by differentiated cells. The experiments were performed in triplicate and 15 fields for each experimental condition were observed (Table IV). Scale bar, 50 μm. MAP2, microtubule-associated protein 2; GFAP, glial fibrillary acid protein; SOX2, sex-determining region Y box 2; GSC, glioma cancer stem cell; DIFF, differentiated.

at 21˚C for 2 h with a horseradish peroxidase-conjugated goat anti-rabbit IgG secondary antibody (cat. no. 12-348; Upstate Biotechnology, Inc., Lake Placid, NY, USA) diluted 1:10,000 in TBSTM. The membranes were rinsed three times in TBST and the luminescence signal was captured using an ImageQuant LAS4000, GE Healthcare (Chicago, IL, USA). Each experiment was performed at least twice.

ELISA nucleosome assay. For the relative quantification of cell death, a colorimetric ELISA sandwich immunoassay was used to detect nucleosomes (Cell Death Detection ELISA; Roche Diagnostics GmbH, Mannheim, Germany). Cells were plated in a 12-well plate and treated with cell culture medium containing 25 μM 1a-RGD for 48 h, in the presence and absence of the caspase inhibitor carbobenzoxy-Val-Ala-Asp-fluoromethylketone (zVAD-fmk; 1 μM). Following incubation, cell lysates were prepared using the lysis buffer supplied in the kit and the assay was performed according to the manufacturer's protocol. Finally, the samples were measured in a multi-well reader at 405 nm. Eight wells were used for each experiment and each experiment was performed three times.

Caspase activity assay. Cells were plated on clear-bottomed 96-well black plates (Costar; Corning Incorporated) at a density of 5,000 cells/well. Caspase-3/7 and -9 activities were determined following the addition of growth medium containing 25 μM 1a-RGD for 48 h, in the presence and absence of the caspase inhibitor zVAD-fmk (1 μM), using Caspase Glo 3/7 and Caspase Glo 9 kits (Promega Corporation). Each experiment was performed in triplicate.

Statistical analysis. Results are expressed as the mean ± standard deviation and analyzed using Student's t-test when comparing two groups or ANOVA and a Tukey's post hoc test for comparing more than two groups. Statistical analyses were performed using GraphPad Prism software (version 5.0; GraphPad Software, Inc., La Jolla, CA, USA). $P<0.05$ was considered to indicate a significant difference.

Results

Characterization of GSC stemness. To characterize and confirm the stemness status of the GSC obtained from specimens from patients with GB, a series of experiments was performed. First, the determination of the stemness markers nestin, MAP2, GFAP and SOX2, in undifferentiated and differentiated GSC was performed by immunostaining (Fig. 1).

When GSC3, normally grown in a serum-free medium, were differentiated using 10% FBS, a statistically significant increase ($P<0.001$) was observed in MAP2- and GFAP-positive cells in comparison with undifferentiated GSC. Conversely, undifferentiated GSC were positive for nestin and SOX2 staining (Table IV). It cannot be excluded that the adhesion conditions on the microscopy glasses may serve a function in inducing slight morphological alterations. However, staining of the markers was consistent and reproducible under all conditions. The immunostaining was also performed in GSC4 and GSC7 lines with similar results (data not shown).

Stemness of GSC confirmed by RT-qPCR. The stemness status of the GSC was confirmed further by the transcriptomic analysis of six stemness markers (9,11) in addition to SOX2 and nestin, in undifferentiated GSC and NHA, used in all experiments as non-tumor reference cells. Except for BMI1 and Nanog, whose expression was similar in the two cell populations, all other stemness marker transcripts exhibited significantly increased expression in GSC compared with in NHA, thus demonstrating that, at least in under the culture conditions used, GSC retained their original stemness status (Fig. 2). In addition, when the analysis was repeated in undifferentiated GSC and in differentiated GSC grown with 10% FBS, the expression of all the transcripts in the latter

Table IV. Cells positive for nestin, MAP2, GFAP and SOX2.

GSC line		Nestin	MAP2	GFAP	SOX2
3	Stem	96 (±2)	18 (±3)	25 (±5)	96 (±5)
	Differentiated	68 (±4)	80 (±4)	89 (±8)	44 (±6)
4	Stem	55 (±5)	5 (±2)	18 (±5)	70 (±5)
	Differentiated	28 (±6)	32 (±8)	34 (±8)	39 (±8)
7	Stem	95 (±3)	44 (±5)	19 (±2)	88 (±6)
	Differentiated	75 (±5)	28 (±5)	74 (±13)	39 (±4)

GSC, glioma cancer stem cell; MAP2, microtubule-associated protein 2; GFAP, glial fibrillary acid protein; SOX2, sex-determining region Y box 2.

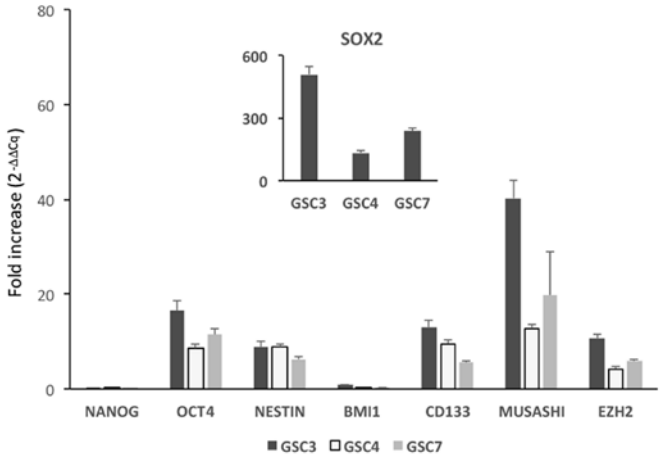

Figure 2. Stemness markers expressed by GSC. mRNA extracted from GSC3, GSC4, GSC7 and NHA was amplified using the reverse transcription-quantitative polymerase chain reaction. ΔΔCq values were determined using RPL6 as a housekeeping gene. Results are expressed as the fold increase ($2^{-\Delta\Delta Cq}$) of selected genes in GSC compared with NHA. The mean RPL6 Cq values were 20.44 for NHA, 16.22 for GSC3, 16.374 for GSC4 and 16.389 for GSC7. GSC, glioma cancer stem cell; NHA, normal human astrocyte; RPL6, ribosomal protein L6.

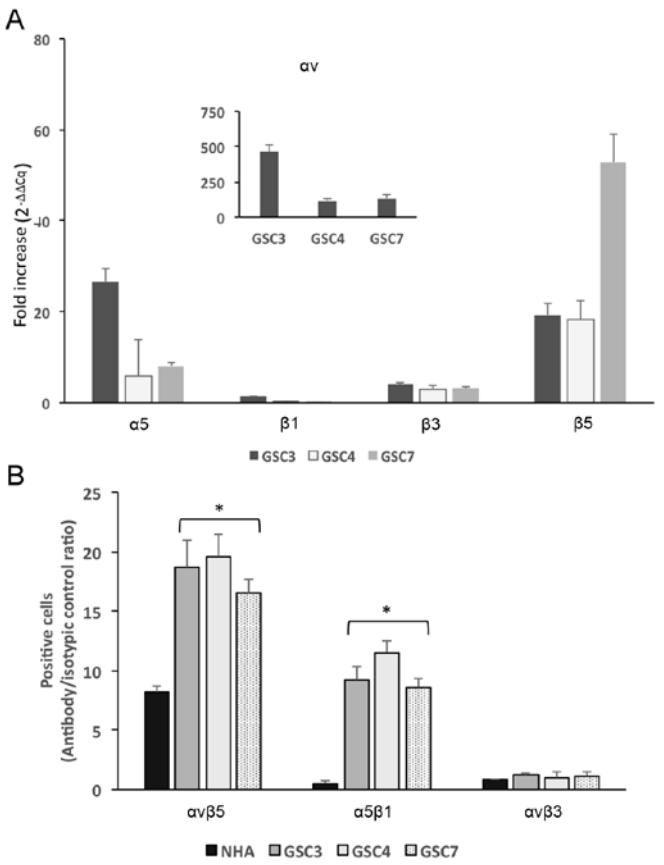

Figure 3. Integrin expression in GSC3, GSC4 and GSC7 lines. (A) mRNA extracted from GSC3, GSC4, GSC7 and NHA was amplified using the reverse transcription-quantitative polymerase chain reaction. Results are expressed as the fold increase ($2^{-\Delta\Delta Cq}$) determined using RPL6 as a housekeeping gene. The mean RPL6 Cq values were 20.44 for NHA, 16.22 for GSC3, 16.374 for GSC4 and 16.389 for GSC7. (B) Flow cytometric analysis was performed on GSC3, GSC4, GSC7 and NHA to assess integrin receptor expression on the cell surface. The cell suspensions were incubated with antibodies recognizing the integrin receptors and >10,000 cells for each experimental point were assessed. Results are expressed as antibody signal/isotypic control ratio. *P<0.05 vs. NHA. GSC, glioma cancer stem cell; NHA, normal human astrocyte; RPL6, ribosomal protein L6.

was significantly lower (data not shown), thus confirming the immunocytochemistry results.

GSC express αv, β3, β5 and α5 integrin subunits. Since previous studies have indicated that some RGD-binding integrins are overexpressed in GB (12), the αvβ3, αvβ5 and α5β1 integrin expression pattern in GSC were investigated by determining the mRNA amounts of αv, β3, β5, α5 and β1 subunits. The RT-qPCR experiments clearly identified that αv, α5 and β5 subunits are overexpressed in all three cell lines examined, compared with the expression profile for NHA (Fig. 3A), with the fold increase ranging between 5 and 500, whereas the expression of β1 and β3 was less pronounced compared with their relative expression in NHA.

To further confirm the integrin receptor expression on GSC membranes, FACS experiments were performed using conjugated fluorescent antibodies recognizing αvβ3, αvβ5 and α5β1 integrins. The expression results, reported as specific signal/isotypic control ratio, are presented in Fig. 3B. The surface expression of αvβ5 and α5β1 integrins was more abundant in GSC compared with in NHA, whereas for αvβ3, no significant difference was identified between GSC and NHA.

These results are in good agreement with the mRNA results from the RT-qPCR assay, and the poor expression of

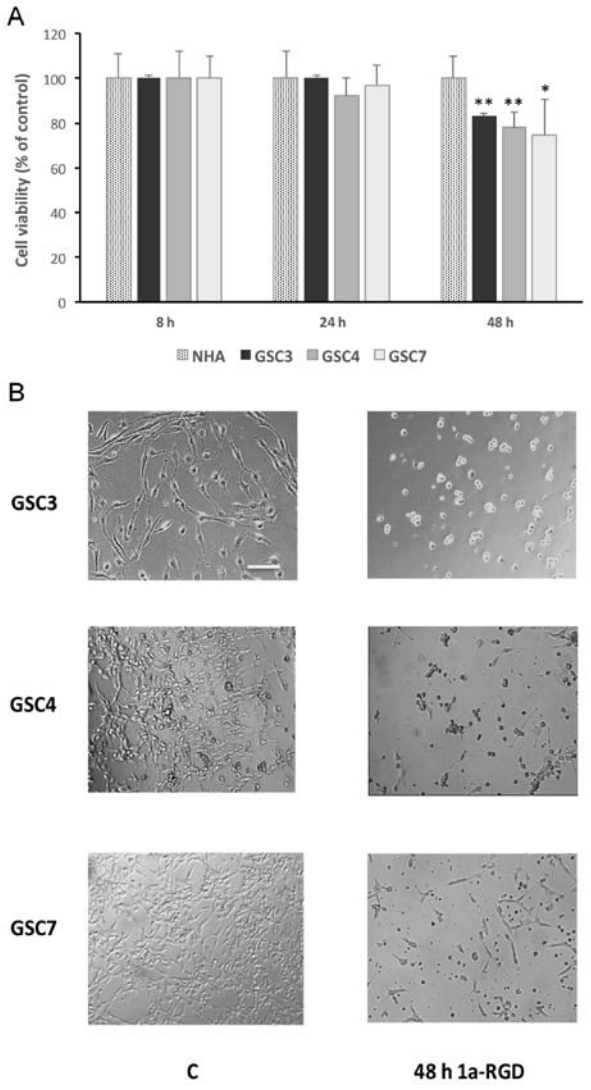

Figure 4. 1a-RGD decreases GSC viability after 48 h. of treatment. (A) The three cell lines were treated for increasing times with 25 μM 1a-RGD and MTS assays were performed. Results are expressed as the mean ± standard deviation cell viability as a percentage of that of the controls. *P<0.05, **P<0.01 vs. NHA. (B) Phase-contrast images of GSC3, GSC4 and GSC7 lines treated for 48 h with 25 μM 1a-RGD. The detached cells assumed the round shape characteristic of cell death. Scale bar, 100 μm. GSC, glioma cancer stem cell; NHA, normal human astrocyte.

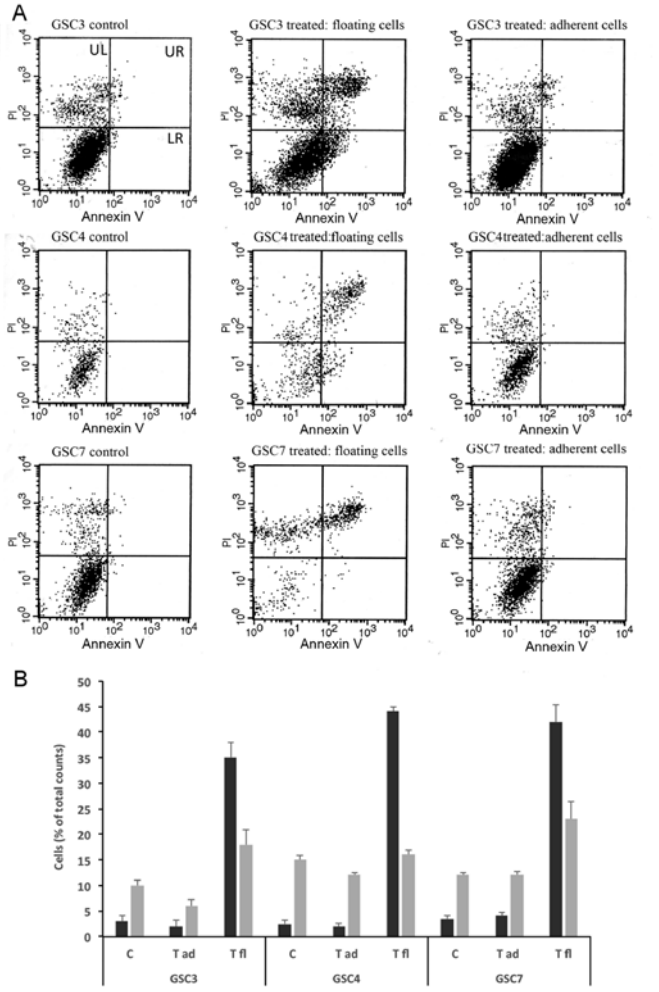

Figure 5. 1a-RGD treatment induces detachment-dependent anoikis. (A) Following treatment with 25 μM 1a-RGD for 48 h, detached and adherent GSC lines from the same wells were separately analyzed by fluorescence-activated cell sorting to assess cell death. (B) Results from flow cytometric analysis. Apoptotic cells were present in the floating fraction, whereas no difference was observed between controls and still adherent treated cells. GSC, glioma cancer stem cell; PI, propidium iodide; UL, upper left; UR, upper right; LL, lower left; LR, lower right; C, controls; T, treated; fl, floating; ad, adherent.

β3 subunit may account for the different integrin expression on the cell surface.

1a-RGD induces cell death in GSC. Since certain discrepancies concerning the effect of RGD antagonists on cancer cells were identified previously (2), the effect of 1a-RGD treatment on GSC viability was determined. In the present study, 1a-RGD was used at a concentration of 25 μM on the basis of its IC_{50} (10.2±0.8 μM), deduced from concentration-response curves performed in GB cell lines (3).

After 48 h of treatment with 1a-RGD, a significant decrease was observed in the viability of GSC that was not replicated in the non-tumorigenic NHA control cells (Fig. 4A). More specifically, following treatment, only GSC were observed to have detached from the plastic dishes. They also exhibited altered morphology, assuming the round shape typical of cells undergoing cell death (Fig. 4B); in contrast, neither cell detachment nor a change in morphology was observed in 1a-RGD-treated NHA (data not shown). These results clearly indicate that 1a-RGD was responsible for the loss of GSC viability, in a process possibly mediated by integrin inhibition.

To verify whether 1a-RGD was responsible for the loss of GSC viability, the extent and type of cell death was investigated separately in adherent and detached cells from the same wells following 1a-RGD treatment (25 μM for 48 h) using an Annexin V/PI FACS assay (Fig. 5A and B). The floating cells and the still adherent cells were collected from each well. Following enumeration, the two fractions were subjected to FACS analysis. Although the three GSC lines exhibited differential sensitivity to the induction of cell death elicited by 1a-RGD, the viability in adherent cells was not significantly different from that observed in untreated cells (controls). In contrast, in detached cells, a marked increase in the number of apoptotic cells was observed, indicating that 1a-RGD causes detachment-induced anoikis in GSC.

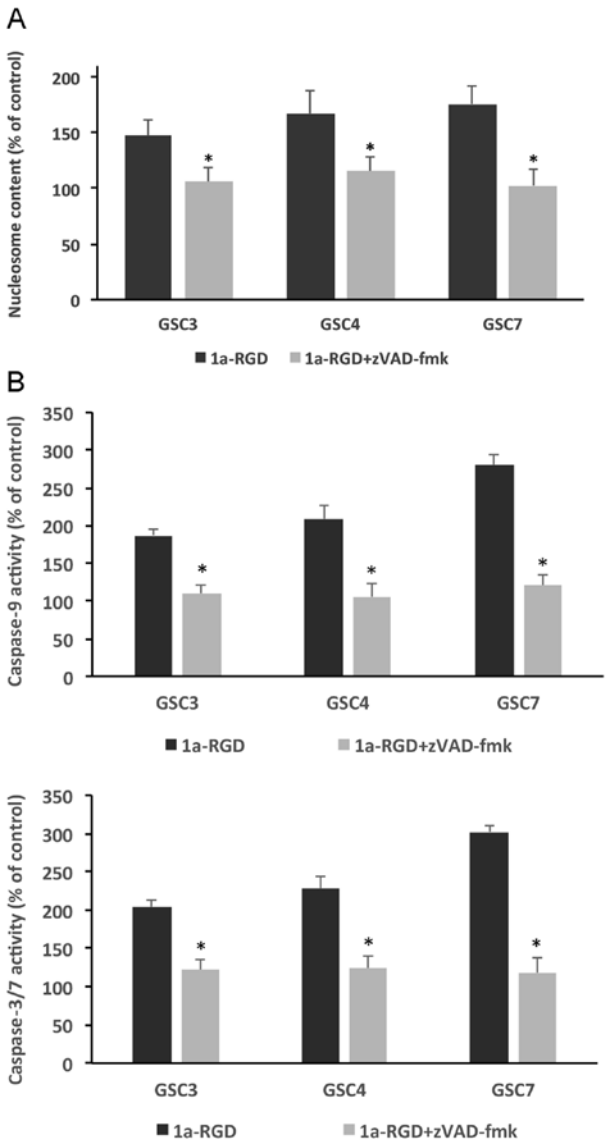

Figure 6. 1a-RGD induces anoikis in a caspase-dependent manner. (A) GSC3, GSC4 and GSC7 lines were treated for 48 h with 25 μM 1a-RGD in the presence or absence of 1 μM zVAD-fmk and ELISAs were performed to determine nucleosome content. All three cell lines following treatment exhibited increased nucleosome content following treatment, whereas incubation with 1 μM zVAD-fmk inhibited nucleosome formation. Results are expressed relative to the controls (vehicle-treated cells). *P<0.05 vs. cells in the absence of zVAD-fmk. (B) In parallel experiments, caspase activity, determined using a fluorimetric assay, was also determined. Caspase activity caused by 1a-RGD was significantly decreased following treatment with 1 μM zVAD-fmk. GSC, glioma cancer stem cell; zVAD-fmk, carbobenzoxy-Val-Ala-Asp-fluoromethylketone.

1a-RGD induces anoikis in GSC via a caspase-dependent mechanism. Under the same experimental conditions, anoikis onset was determined using two different assays: A nucleosome ELISA assay and a caspase-3/7 activity assay. Treating the cells for 48 h with 25 μM 1a-RGD induced a significant increase in nucleosome content compared with control samples in all three GSC examined; notably, this increase was partially rescued by incubating GSC with 1 μM zVAD-fmk, thus suggesting that caspase-3/7 mediate, at least in part, this anoikis-associated process (Fig. 6A).

This supposed function of caspase-3/7 in sustaining anoikis was further confirmed using a fluorimetric caspase activity assay performed under the same experimental conditions. Similar to that observed using the nucleosome assay, the increase in caspase-3/7 activity observed in 1a-RGD-treated GSC was significantly blunted by the caspase inhibitor zVAD-fmk (Fig. 6B), thus confirming that the observed anoikis was indeed dependent on caspase-3/7 activation.

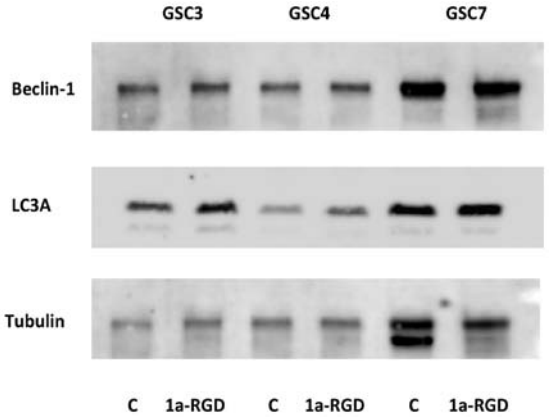

Figure 7. Autophagy is not involved in 1a-RGD-induced anoikis. Following treatment with 25 μM 1a-RGD for 48 h, cell lysates from GSC3, GSC4 and GSC7 lines were analyzed by western blotting. Beclin-1 and LC3A content was the same in treated cells as in controls. α-tubulin was used as a loading control. GSC, glioma cancer stem cell; LC3, light chain 3.

1a-RGD-induced anoikis is not sustained by autophagy. Since integrin inhibition has been identified to induce atypical anoikis in glioma cells (13), the possibility that anoikis elicited by integrin inhibition via 1a-RGD may involve processes associated with autophagy in GSC was investigated.

GSC were exposed to 25 μM 1a-RGD for 48 h, and cell lysates were subjected to electrophoresis and western blotting (Fig. 7). There were no changes in total levels of light chain 3 (LC3)-II and beclin-1, two proteins associated with the induction of autophagy (14), suggesting that, in the present study, cell death was due to caspase-dependent anoikis, with no apparent contribution from autophagy-associated processes.

1a-RGD inhibits focal adhesion kinase (FAK) and protein kinase B (Akt) phosphorylation. The interaction with integrins of several endogenous ECM proteins leads to the activation of a variety of downstream protein kinases, such as FAK, extracellular-signal-regulated kinase (ERK) and Akt (2,3). To investigate whether 1a-RGD interferes with the activation of these signaling pathways, western blot analysis was used to determine the effect of 25 μM 1a-RGD treatment on the phosphorylation state of these downstream kinases. It was identified that 1a-RGD treatment for 48 h significantly decreases FAK and Akt phosphorylation (Fig. 8A and B), whereas ERK phosphorylation was not affected (data not shown); a shorter treatment (8 h) of GSC with 1a-RGD did not affect the phosphorylation state of the two kinases (data not shown).

1a-RGD decreases GSC migration. The features of GSC most implicated in their malignancy are their ability to disseminate, along with their potential invasiveness into the surrounding parenchyma. Since, in some cellular models, the

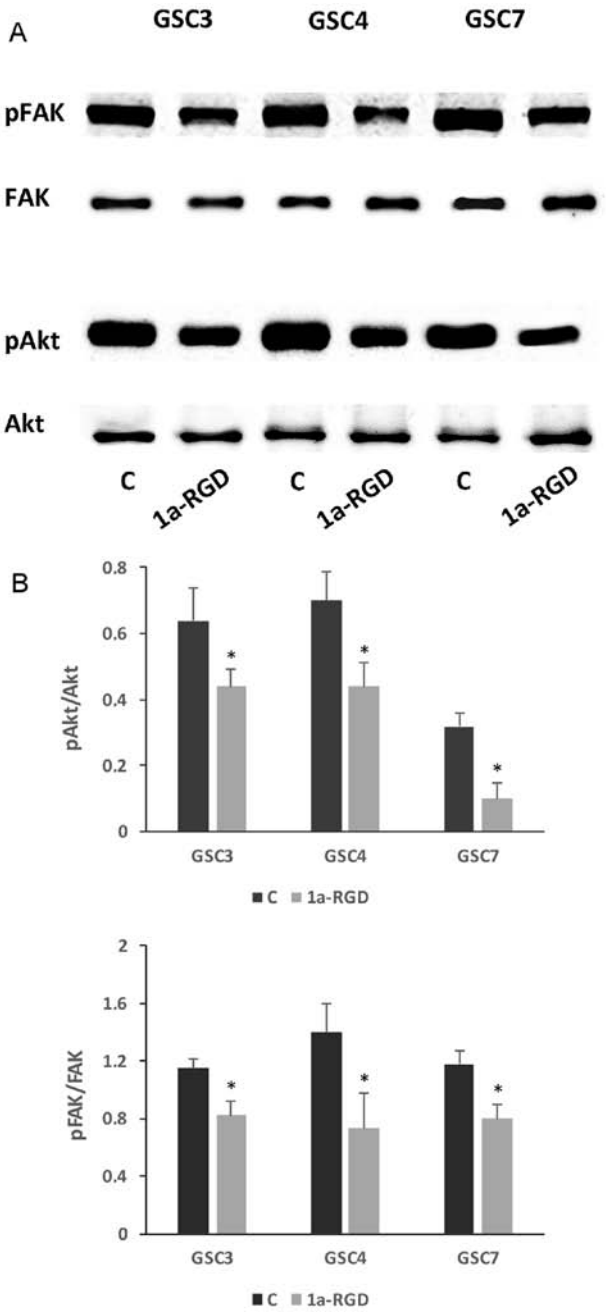

Figure 8. 1a-RGD decreases FAK and Akt phosphorylation. (A) Following treatment with 25 μM 1a-RGD for 48 h, cell lysates were analyzed by western blotting using anti-pFAK and anti-pAkt antibodies. Markedly weaker phosphorylation signals were observed in GSC3, GSC4 and GSC7 lines for FAK and Akt. (B) Densitometric analysis of pAkt and pFAK western blot experiments, normalized to the relative total (unphosphorylated + phosphorylated) proteins. *P<0.05 vs. controls. FAK, focal adhesion kinase; Akt, protein kinase B; ERK, extracellular-signal-regulated kinase; p, phospho-; GSC, glioma cancer stem cell; C, control.

integrin-dependent inhibition of downstream FAK and Akt pathways is functionally associated with a decrease in cell motility, it was investigated whether 1a-RGD affects GSC migration in the experimental model.

A Transwell chamber assay was performed using EGF and bFGF as chemoattractant. Treatment with 25 μM 1a-RGD for 8 h resulted in significantly decreased numbers of migratory cells in all three GSC tested, compared with controls. Notably, this inhibitory effect was not observed in NHA (Fig. 9),

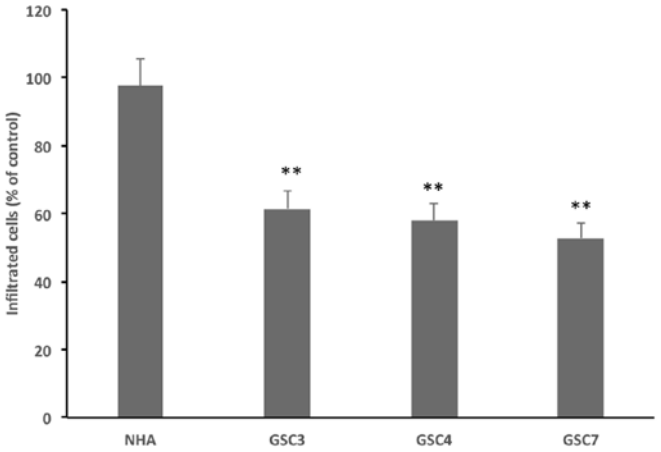

Figure 9. 1a-RGD inhibits GSC migration. Cells plated in Transwells were treated with 25 μM 1a-RGD for 8 h. Migratory cells were enumerated using fluorescence microscopy. **P<0.01 vs NHA. GSC, glioma cancer stem cell; NHA, normal human astrocyte.

possibly due to the lower integrin expression in these non-tumoral cells, as aforementioned.

Discussion

Integrins are an appealing potential target in cancer biology because they mediate crucial features of tumor malignancy, i.e. detachment from the original tumoral mass, metastatic dissemination and the invasion of distant sites, which culminate in the formation of a new tumoral niche (15,16). Disappointing results from early clinical studies, employing the canonical prototype integrin-binding molecule cilengitide have stimulated attempts to synthesize and exploit the pharmacological properties of other RGD-containing molecules with different chemical structures (2). This approach appears to be particularly suitable for GB because tumor cells themselves and those belonging to the tumor niche overexpress RGD-binding integrins. In addition, the strategy of targeting integrins may impair the dissemination of glioma cancer stem cells, responsible for the fatal relapses observed following surgery in patients with glioma (17). Also, in a recent study, $\alpha v\beta 3$ integrin has been identified as an effective target for cilengitide in a subset of GBM (18).

Studies performed using *in vitro* models of mouse and human glioma cell lines have identified that several RGD-containing integrin antagonists affect cell viability, apoptosis and sensitize glioma cells to alkylating drugs (3,19). However, in these studies, glioma cell lines were grown and maintained in the presence of serum, a condition that may alter the original phenotype of the tumor tissue. To partially overcome this drawback in the present study, the stemness properties were initially characterized, together with the expression of RGD-binding integrin subunits, of GSC grown under adherent conditions and in the absence of serum. Following validation of the model, the effects of an RGD integrin antagonist, 1a-RGD, on cell viability, cell migration and cell death mechanisms in GSC were investigated.

In agreement with a previous study (20), the results of the present study identified that GSC grown on laminin-coated

plastic, in the presence of the growth factors EGF and bFGF and neurobasal medium, retain their stemness features *in vitro* and give rise to brain tumors when implanted in a rodent model. Quantitative analysis of stemness markers by RT-qPCR clearly demonstrated that the transcript levels of these markers were more abundant than in differentiated NHA, confirming that stemness of the brain tumor cell population was retained under the experimental conditions used.

The use of suitable and reliable control cells when comparing the expression of specific biomarkers in GSC is currently, for several theoretical and technical reasons, a much-debated and controversial issue that has been poorly addressed in the literature.

Primary cultures of astrocytes represent a valuable tool to study their function in health and disease (21). Human astrocytes grown and propagated *in vitro* may be obtained primarily from three sources: i) Primary fetal astrocytes sometimes considered the current 'gold standard' (22); ii) human induced pluripotent stem cell-derived astrocytes (23); and iii) acutely purified astrocytes from fetal and adult human brain obtained using an immunopanning-based technique using an antibody targeting hepatic and glial cell adhesion molecule (or glial cell adhesion molecule), a surface protein expressed by human astrocytes, to generate highly purified (>95%) cultures of primary human astrocytes (24) maintained under serum-free conditions. However, currently, a detailed comparison among human *in vitro* astrocytes obtained from different sources remains lacking and it is therefore impossible to determine which model is preferable. Furthermore, all cell culture systems have intrinsic problems, since no culture system can fully replicate the *in vivo* conditions. It is remarkable that Zhang *et al* (24) identified that human astrocytes exist in two distinct developmental stages: A fetal highly proliferative astrocyte precursor cell and a mature post-mitotic astrocyte. The advantage of using fetal astrocytes is associated with the fact that they can be purchased commercially, and can be frozen, stored and defrosted at a later time for subsequent experiments. However, on the basis of these premises, we are well aware of the limitations of using fetal astrocytes (NHA) as normal control in studies with GSC, but we also consider that they currently represent the most accessible source of human astrocytes. Therefore, future studies aimed at comparing the features of human astrocytes propagated *in vitro* and obtained from different sources are mandatory to assess which cellular model should be adopted as a proper control in studies involving GSC.

Another notable result obtained in the present study concerns the expression of integrins in GSC: The majority of data available in the literature concerning the expression of RGD-binding integrins were obtained using glioma cell lines grown in the presence of serum, a condition that may not reflect the genotype of cell populations present in the original brain tumor (25). In agreement with previous studies describing the overexpression of RGD-binding integrins in glioma cells and tumor specimens (12), the results of the present study indicated that GSC overexpressed the αv, β5 and α5 integrin subunit transcripts compared with NHA, whereas no difference was identified in the level of β3 transcript. These results were confirmed by FACS analysis of integrin expression on GSC membranes, suggesting that the low β3 expression may be the limiting step for αvβ3 receptor expression.

Previous studies identified that cilengitide induced detachment-mediated anoikis in pediatric glioma and neuroblastoma cell lines (26), inhibited proliferation and promoted apoptosis via downregulation of FAK-, Src- and Akt-dependent pathways in glioma cells (27), and in glioma cancer cells triggered antiapoptotic autophagy mechanisms that sustained detachment-dependent atypical anoikis (13). However, the function of autophagy in regulating cell death in glioma cells is controversial and appears to be strictly associated with the type of cell examined and to the culture conditions, because it has been identified that, in glioma cell lines, autophagy was enhanced and supported cell death, acting as a pro-apoptotic element (28).

The results of the presents study clearly indicate that 1a-RGD induces detachment-mediated anoikis in GSC and that the contribution, if any, of other cell-death-associated mechanisms, such as necrosis and autophagy, appears to be marginal and limited.

Three separate lines of evidence from the present study support this conclusion. First, the cells that remained attached to the wells after 48 h of treatment with 1a-RGD were viable, whereas most of the detached cells had undergone cell death. Secondly, analysis of the detached cells by FACS/Annexin V staining exhibited no increase in the necrotic index in treated cells compared with untreated cells. Finally, the levels of two autophagy markers, LC3 and Beclin-1 (14,28), were not modified in detached cells following 1a-RGD treatment.

It was also identified that caspase activity, together with nucleosome formation, was markedly decreased when GSC were simultaneously treated with the pan-caspase inhibitor zVAD-fmk, clearly indicating that the type of anoikis observed in GSC required caspase-3/7 and caspase-9 activation. This result is in contrast with those of Silginer *et al* (13), which described atypical caspase-independent anoikis induced by cilengitide in human and mouse glioma cancer cells (13). Several experimental factors, such as different integrin subtype expression patterns and the pharmacological profile of the integrin antagonists used, may account for the differences in the reported mechanisms leading to cell death. The results of the present study indicate that autophagy is not involved in 1a-RGD-induced anoikis; nevertheless, no firm conclusions can be drawn, and the function of autophagy in cell death processes and GB dissemination clearly requires further investigation.

Integrin-dependent regulation of cellular effects such as survival, growth, migration and resistance to anoikis are mediated by FAK activation by two distinct, but not mutually exclusive, mechanisms: Activation of phosphoinositide 3-kinase (PI3K)/Akt- and ERK-dependent signaling pathways and regulation of the crosstalk between integrins and growth factor receptor signaling (29).

The results of western blot experiments, obtained using anti-phospho-specific antibodies, indicate that the FAK- and Akt-dependent pathways are likely to serve a significant function in 1a-RGD-dependent anoikis induction and inhibition of cell migration. The experiments of the present study were performed in the presence of 25 μM 1a-RGD for 24 h: In other experiments, it has not been possible to detect

significant p (phospho-)Akt and pFAK signal decreases in GSC following shorter treatment times (for example, 8-h treatment; data not shown). We hypothesize that a contact time <24 h is insufficient to reveal a change in the phosphorylation status of these proteins; indeed, FAK and Akt are the convergence point for a number of distinct signaling pathways and therefore a slight decrease in their phosphorylation state may be difficult to detect, being masked by concomitant stimulation from other receptors, such as growth factor receptors.

Similar mechanisms have been described for other cell types: In fibroblasts, the activation of β1 integrin triggers a viability signal, mediated by the activation of a FAK/PI3K/Akt-dependent signaling pathway, that protects cells from apoptosis (30), and in human intestinal epithelial cells, the suppression of anoikis requires a selective repertoire of integrins to activate the FAK/Src-dependent pathway (31). The relevance of FAK inhibition as a key event in anoikis resistance has recently been highlighted in an elegant study (32) in which it was revealed that internalized integrins trigger the assembly of endosomal signaling complexes which, in turn, recruit FAK and induce anoikis resistance, thereby promoting cancer cell survival and metastatic growth. Further studies on GSC, aimed at dissecting the specific mechanism by which integrin antagonists counteract anoikis resistance, are therefore required to understand the potential function of SMIA in limiting GSC dissemination.

The inhibition of GSC migration is an intriguing result, particularly because targeting the ability of GSC to infiltrate distant brain areas, via brain parenchyma or brain vessels (2), is possibly the primary issue in limiting glioma malignancy. This issue has been investigated previously (33) Although we did not investigate in detail the molecular mechanisms involved in the observed inhibition of cell migration induced by 1a-RGD, a previous study identified that an RGD-integrin antagonist and a blocking antibody directed against αβ subunits decreased the pro-migratory effect elicited by transforming growth factor β (TGF-β) in human glioma cell lines (34). This mechanism is possibly the one that occurred in our experimental model: In other experiments of the present study not described, GSC were identified to express abundant levels of TGF-β and TGF-β-receptor mRNAs, suggesting the existence of an autocrine TGF-β-dependent mechanism mediating several important cellular effects.

In this scenario, we hypothesize that, in our model, 1a-RGD may therefore decrease cell migration by inhibiting the release of free active TGF-β from its ternary complex, as has been identified to occur in other cellular systems (35).

In conclusion, the results of the present study indicate that GSC grown under adherent conditions are a suitable model for investigating the interactions between integrins and SMIA as well as the molecular mechanisms that underlie the functional consequences elicited by this interaction. In addition, the results of the present study identified that the integrin antagonist 1a-RGD induces detachment-mediated caspase-dependent anoikis and markedly inhibits the migration of GSC, supporting the possibility, to be investigated in future studies in *in vivo* and *in vitro* models, that SMIA may be a useful tool for promoting anoikis in GSC, and thus for limiting the intracranial dissemination of glioma cells.

Acknowledgements

Not applicable.

Funding

The present study was supported by the Italian Ministry for University and Research by Project of Relevant National Interest 2015 (grant no. 20157WW5EH_006).

Availability of data and materials

All data generated or analyzed during this study are included in this published article.

Authors' contributions

MP designed the research project and performed part of the experiments; MCG performed part of the experiments and contributed to the experimental design; AD isolated GSC from glioma specimen and characterized the cells performing tumorigenicity and immunocytochemistry experiments; EC performed flow cytometry experiments; MS and LC synthesized 1a-RGD; SS co-ordinated the research activity, contributed to the experimental design and was involved in drafting the manuscript and revising it critically.

Ethics approval and consent to participate

Tumor tissues were obtained from the Neurosurgery Department at the Institute for Research, Hospitalization and Care-University Hospital (IRCCS) San Martino-Cancer Research Institute (IST) (Genoa, Italy) following informed consent, according to European Union legislation on informed consent and The Declaration of Helsinki, from the patients and Institutional Ethical Committee (IRCCS San Martino-IST) approval. All experiments involving animals were performed at IRCCS-AOU San Martino-IST in compliance with the guidelines approved by the Italian Ministry of Health and the Committee for Animal Well-Being in Cancer Research.

Patient consent for publication

Not applicable.

Competing interests

The authors have no conflict of interests to declare.

References

1. Pollard SM, Yoshikawa K, Clarke ID, Danovi D, Stricker S, Russell R, Bayani J, Head R, Lee M, Bernstein M, *et al*: Glioma stem cell lines expanded in adherent culture have tumor-specific phenotypes and are suitable for chemical and genetic screens. Cell Stem Cell 4: 568-580, 2009.
2. Paolillo M, Serra M and Schinelli S: Integrins in glioblastoma: Still an attractive target? Pharmacol Res 113A: 55-61, 2016.
3. Russo MA, Paolillo M, Sanchez-Hernandez Y, Curti D, Ciusani E, Serra M, Colombo L and Schinelli S: A small-molecule RGD-integrin antagonist inhibits cell adhesion, cell migration and induces anoikis in glioblastoma cells. Int J Oncol 42: 83-92, 2013.

4. Panzeri S, Zanella S, Arosio D, Vahdati L, Dal Corso A, Pignataro L, Paolillo M, Schinelli S, Belvisi L, Gennari C, *et al*: Cyclic isoDGR and RGD peptidomimetics containing bifunctional diketopiperazine scaffolds are integrin antagonists. Chemistry 21: 6265-6271, 2015.
5. Cheng NC, van Zandwijk N and Reid G: Cilengitide inhibits attachment and invasion of malignant pleural mesothelioma cells through antagonism of integrins αvβ3 and αvβ5. PLoS One 9: e90374, 2014.
6. Mikheev AM, Mikheeva SA, Trister AD, Tokita MJ, Emerson SN, Parada CA, Born DE, Carnemolla B, Frankel S, Kim DH, *et al*: Periostin is a novel therapeutic target that predicts and regulates glioma malignancy. Neuro-oncol 17: 372-382, 2015.
7. Arosio D, Belvisi L, Colombo L, Colombo M, Invernizzi D, Manzoni L, Potenza D, Serra M, Castorina M, Pisano C, *et al*: A potent integrin antagonist from a small library of cyclic RGD pentapeptide mimics including benzyl-substituted azabicycloalkane amino acids. ChemMedChem 3: 1589-1603, 2008.
8. Carra E, Barbieri F, Marubbi D, Pattarozzi A, Favoni RE, Florio T and Daga A: Sorafenib selectively depletes human glioblastoma tumor-initiating cells from primary cultures. Cell Cycle 12: 491-500, 2013.
9. Lee KH, Ahn EJ, Oh SJ, Kim O, Joo YE, Bae JA, Yoon S, Ryu HH, Jung S, Kim KK, *et al*: KITENIN promotes glioma invasiveness and progression, associated with the induction of EMT and stemness markers. Oncotarget 6: 3240-3253, 2015.
10. Livak KJ and Schmittgen TD: Analysis of relative gene expression data using real-time quantitative PCR and the 2(-Δ Δ C(T)) Method. Methods 25: 402-408, 2001.
11. Hadjimichael C, Chanoumidou K, Papadopoulou N, Arampatzi P, Papamatheakis J and Kretsovali A: Common stemness regulators of embryonic and cancer stem cells. World J Stem Cells 7: 1150-1184, 2015.
12. Desgrosellier JS and Cheresh DA: Integrins in cancer: Biological implications and therapeutic opportunities. Nat Rev Cancer 10: 9-22, 2010.
13. Silginer M, Weller M, Ziegler U and Roth P: Integrin inhibition promotes atypical anoikis in glioma cells. Cell Death Dis 5: e1012, 2014.
14. Mizushima N and Yoshimori T: How to interpret LC3 immunoblotting. Autophagy 3: 542-545, 2007.
15. Seguin L, Desgrosellier JS, Weis SM and Cheresh DA: Integrins and cancer: Regulators of cancer stemness, metastasis, and drug resistance. Trends Cell Biol 25: 234-240, 2015.
16. Buchheit CL, Weigel KJ and Schafer ZT: Cancer cell survival during detachment from the ECM: Multiple barriers to tumour progression. Nat Rev Cancer 14: 632-641, 2014.
17. Beier D, Schulz JB and Beier CP: Chemoresistance of glioblastoma cancer stem cells--much more complex than expected. Mol Cancer 10: 128, 2011.
18. Cosset É, Ilmjärv S, Dutoit V, Elliott K, von Schalscha T, Camargo MF, Reiss A, Moroishi T, Seguin L, Gomez G, *et al*: Glut3 addiction is a druggable vulnerability for a molecularly defined subpopulation of glioblastoma. Cancer Cell 32: 856-868.e5, 2017.
19. Christmann M, Diesler K, Majhen D, Steigerwald C, Berte N, Freund H, Stojanović N, Kaina B, Osmak M, Ambriović-Ristov A, *et al*: Integrin αVβ3 silencing sensitizes malignant glioma cells to temozolomide by suppression of homologous recombination repair. Oncotarget 8: 27754-27771, 2017.
20. Rahman M, Reyner K, Deleyrolle L, Millette S, Azari H, Day BW, Stringer BW, Boyd AW, Johns TG, Blot V, *et al*: Neurosphere and adherent culture conditions are equivalent for malignant glioma stem cell lines. Anat Cell Biol 48: 25-35, 2015.
21. Lange SC, Bak LK, Waagepetersen HS, Schousboe A and Norenberg MD: Primary cultures of astrocytes: Their value in understanding astrocytes in health and disease. Neurochem Res 37: 2569-2588, 2012.
22. Malik N, Wang X, Shah S, Efthymiou AG, Yan B, Heman-Ackah S, Zhan M and Rao M: Comparison of the gene expression profiles of human fetal cortical astrocytes with pluripotent stem cell derived neural stem cells identifies human astrocyte markers and signaling pathways and transcription factors active in human astrocytes. PLoS One 9: e96139, 2014.
23. Lundin A, Delsing L, Clausen M, Ricchiuto P, Sanchez J, Sabirsh A, Ding M, Synnergren J, Zetterberg H, Brolén G, *et al*: Human iPS-derived astroglia from a stable neural precursor state show improved functionality compared with conventional astrocytic models. Stem Cell Reports 10: 1030-1045, 2018.
24. Zhang Y, Sloan SA, Clarke LE, Caneda C, Plaza CA, Blumenthal PD, Vogel H, Steinberg GK, Edwards MS, Li G, *et al*: Purification and characterization of progenitor and mature human astrocytes reveals transcriptional and functional differences with mouse. Neuron 89: 37-53, 2016.
25. Lee J, Kotliarova S, Kotliarov Y, Li A, Su Q, Donin NM, Pastorino S, Purow BW, Christopher N, Zhang W, *et al*: Tumor stem cells derived from glioblastomas cultured in bFGF and EGF more closely mirror the phenotype and genotype of primary tumors than do serum-cultured cell lines. Cancer Cell 9: 391-403, 2006.
26. Leblond P, Dewitte A, Le Tinier F, Bal-Mahieu C, Baroncini M, Sarrazin T, Lartigau E, Lansiaux A and Meignan S: Cilengitide targets pediatric glioma and neuroblastoma cells through cell detachment and anoikis induction. Anticancer Drugs 24: 818-825, 2013.
27. Oliveira-Ferrer L, Hauschild J, Fiedler W, Bokemeyer C, Nippgen J, Celik I and Schuch G: Cilengitide induces cellular detachment and apoptosis in endothelial and glioma cells mediated by inhibition of FAK/src/AKT pathway. J Exp Clin Cancer Res 27: 86, 2008.
28. Antonioli M, Di Rienzo M, Piacentini M and Fimia GM: Emerging mechanisms in initiating and terminating autophagy. Trends Biochem Sci 42: 28-41, 2017.
29. Bianconi D, Unseld M and Prager GW: Integrins in the spotlight of cancer. Int J Mol Sci 17: 2037-2064, 2016.
30. Xia H, Nho RS, Kahm J, Kleidon J and Henke CA: Focal adhesion kinase is upstream of phosphatidylinositol 3-kinase/Akt in regulating fibroblast survival in response to contraction of type I collagen matrices via a beta 1 integrin viability signaling pathway. J Biol Chem 279: 33024-33034, 2004.
31. Beauséjour M, Thibodeau S, Demers MJ, Bouchard V, Gauthier R, Beaulieu JF and Vachon PH: Suppression of anoikis in human intestinal epithelial cells: Differentiation state-selective roles of α2β1, α3β1, α5β1, and α6β4 integrins. BMC Cell Biol 14: 53, 2013.
32. Alanko J, Mai A, Jacquemet G, Schauer K, Kaukonen R, Saari M, Goud B and Ivaska J: Integrin endosomal signalling suppresses anoikis. Nat Cell Biol 17: 1412-1421, 2015.
33. Niola F, Zhao X, Singh D, Sullivan R, Castano A, Verrico A, Zoppoli P, Friedmann-Morvinski D, Sulman E, Barrett L, *et al*: Mesenchymal high-grade glioma is maintained by the ID-RAP1 axis. J Clin Invest 123: 405-417, 2013.
34. Platten M, Wick W, Wild-Bode C, Aulwurm S, Dichgans J and Weller M: Transforming growth factors beta(1) (TGF-beta(1)) and TGF-beta(2) promote glioma cell migration via Up-regulation of alpha(V)beta(3) integrin expression. Biochem Biophys Res Commun 268: 607-611, 2000.
35. Parvani JG, Galliher-Beckley AJ, Schiemann BJ and Schiemann WP: Targeted inactivation of β1 integrin induces β3 integrin switching, which drives breast cancer metastasis by TGF-β. Mol Biol Cell 24: 3449–3459, 2013.